Eur. J. Biochem. **270**, 849–860 (2003) © FEBS 2003 doi:10.1046/j.1432-1033.2003.03441.x

On the molecular basis of the recognition of angiotensin II (AII)

NMR structure of AII in solution compared with the X-ray structure of AII bound to the mAb Fab131

Andreas G. Tzakos[1], Alexandre M. J. J. Bonvin[2], Anasstasios Troganis[3], Paul Cordopatis[4], Mario L. Amzel[5], Ioannis P. Gerothanassis[1] and Nico A. J. van Nuland[2]

[1]*Department of Chemistry, Section of Organic Chemistry and Biochemistry, University of Ioannina, GR-45110, Greece,* [2]*Bijvoet Center for Biomolecular Research, Department of NMR Spectroscopy, Utrecht, the Netherlands;* [3]*Department of Biological Applications and Technologies, University of Ioannina, Greece;* [4]*Department of Pharmacy, University of Patras, Greece;* [5]*Department of Biophysics and Biophysical Chemistry, Johns Hopkins University, School of Medicine, Baltimore, MD 21205, USA*

The high-resolution 3D structure of the octapeptide hormone angiotensin II (AII) in aqueous solution has been obtained by simulated annealing calculations, using high-resolution NMR-derived restraints. After final refinement in explicit water, a family of 13 structures was obtained with a backbone RMSD of 0.73 ± 0.23 Å. AII adopts a fairly compact folded structure, with its C-terminus and N-terminus approaching to within ≈ 7.2 Å of each other. The side chains of Arg2, Tyr4, Ile5 and His6 are oriented on one side of a plane defined by the peptide backbone, and the Val3 and Pro7 are pointing in opposite directions. The stabilization of the folded conformation can be explained by the stacking of the Val3 side chain with the Pro7 ring and by a hydrophobic cluster formed by the Tyr4, Ile5 and His6 side chains. Comparison between the NMR-derived structure of AII in aqueous solution and the refined crystal structure of the complex of AII with a high-affinity mAb (Fab131) [Garcia, K.C., Ronco, P.M., Verroust, P.J., Brunger, A.T., Amzel, L.M. (1992) *Science* **257**, 502–507] provides important quantitative information on two common structural features: (a) a U-shaped structure of the Tyr4-Ile5-His6-Pro7 sequence, which is the most immunogenic epitope of the peptide, with the Asp1 side chain oriented towards the interior of the turn approaching the C-terminus; (b) an Asx-turn-like motif with the side chain aspartate carboxyl group hydrogen-bonded to the main chain NH group of Arg2. It can be concluded that small rearrangements of the epitope 4–7 in the solution structure of AII are required by a mean value of 0.76 ± 0.03 Å for structure alignment and ≈ 1.27 ± 0.02 Å for sequence alignment with the X-ray structure of AII bound to the mAb Fab131. These data are interpreted in terms of a biological 'nucleus' conformation of the hormone in solution, which requires a limited number of structural rearrangements for receptor–antigen recognition and binding.

Keywords: angiotensin II; monoclonal antibody; NMR; peptide structure; VIb turn.

Angiotensin II (AII), the main effector octapeptide hormone (Asp1-Arg2-Val3-Tyr4-Ile5-His6-Pro7-Phe8) of the renin–angiotesin system [1], exerts a variety of actions on different target organs via specific receptors designated AT_1 and AT_2 [2,3]. Most of the known physiological effects of AII have been attributed to AT_1, e.g. vasoconstriction, aldosterone release, renal sodium reabsorption, as well as central osmoregulatory actions, including the release of pituitary hormones into the circulation and growth stimulation in various cell types. These effects constitute the role of angiotensin peptides as neuromodulators/neurotransmitters in the brain. Because of the variety of biological and physiological actions of AII in various tissues, intensive research is required to determine the structural features of this phylogenetic hormone. This should provide the structural basis for the biological pathway of conformation–information–transformation.

For peptide ligand–receptor interactions, there are three general approaches that can be utilized to extract structural information [4]: a peptide (ligand)-based approach, a receptor-based approach, and approaches that target the ligand–receptor complex. In many systems of biological importance, structural characterization of the receptor, and peptide–receptor complexes, is extremely difficult. This is especially true for the membrane-associated G-protein (guanine nucleotide-binding regulatory protein)-coupled receptors, through which AII and most peptide hormones exert their biological activity [5]. Structural determination of these proteins has progressed slowly [6], mainly because of technical difficulties in purifying and handling integral membrane proteins. The instability of these proteins in environments lacking phospholipids and the tendency for them to aggregate and precipitate has hindered application

Correspondence to I. P. Gerothanassis, Department of Chemistry, Section of Organic Chemistry and Biochemistry, University of Ioannina, Ioannina GR-45110, Greece.
Fax: + 30651098799, Tel.: + 30651098397,
E-mail: igeroth@cc.uoi.gr; URL: www.uoi.gr

Abbreviations: AII, angiotensin II; AT_1, AII receptor type 1; CSD, chemical shift deviation.

(Received 3 September 2002, revised 9 December 2002, accepted 20 December 2002)

of standard structure determination techniques to these biomolecules.

In the free ligand (peptide)-based approach, the conformational distribution of the peptide hormone, such as AII, in solution is investigated, on the grounds that this parameter is involved in their binding to the receptor. As a corollary of this argument, it has often been assumed that the conformation of the hormone in the complex corresponds to the predominant conformation in solution according to the key-to-lock model. However, an alternative molecular recognition process, the so-called 'zipper' model, has been suggested in several instances [7–11]. The key question therefore is whether structural motifs of a flexible peptide ligand in solution can be retained during the early stages of receptor–peptide recognition processes [12].

AII has been extensively investigated in solution during the last 40 years with a variety of techniques, including theoretical, physicochemical, and spectroscopic. The results have been interpreted in terms of various models such as an α-helix [13], β-turn [14–17], cross-β-forms II [18], antiparallel pleated sheet [19,20], γ-turn [19], random coil [21,22], inverse γ-turn [23], side chain ring cluster [24], and other structures [25–29]. It is evident that several of the reported models are not consistent with each other and that there is no general consensus on the solution conformation of AII.

Here we present detailed high-field 2D ^{1}H-^{1}H TOCSY and 2D ^{1}H-^{1}H NOESY NMR studies of AII, at low temperature (≈ 277 K) in aqueous solution, at neutral pH (≈ 5.7). The high-resolution structures, calculated from NMR-derived restraints, provide the first experimental evidence that the hormone adopts a U-shaped (VIb turn) folded structure. The conformational features of AII in the solution state (representing the free ligand conformation) were compared with the conformation of the hormone complexed to the high-affinity mAb Fab131 (representing the receptor-bound conformation) as determined by X-ray crystallography [30]. This antibody has the unusual property that it was not generated against AII, but rather against an anti-idiotypic Ig with a mAb to AII, which renders this antibody an anti-(anti-idiotypic) Ig. The high affinity for AII of the original mAb was passed on to mAb131 through structural determinants on the anti-idiotypic Ig.

Materials and methods

Peptide synthesis and sample preparation

AII was synthesized according to a standard stepwise solid-phase procedure using Fmoc/tBu chemistry [31,32]. Peptide purity was assessed by analytical HPLC (Nucleosil-120 C_{18}; reversed phase; 250 × 4.0 mm), mass spectrometry (FABMS, ESIMS), and amino-acid analysis. The samples were prepared for NMR spectroscopy by dissolving the peptide in 0.01 M potassium phosphate buffer (pH 5.7), containing 0.02 M KCl. 2,2-Dimethyl-2-silapentanesulfonate (DSS) was added to a concentration of 1 mM as an internal chemical shift reference. Peptide concentration was commonly 4 mM in 90% $^{1}H_2O$/10% $^{2}H_2O$. Trace amounts of NaN_3 were added as a preservative.

NMR spectroscopy: determination of distance restraints

Preliminary NMR spectra were acquired at 400 MHz using a Bruker AMX-400 spectrometer in the NMR Center of the University of Ioannina. High-field NMR spectra were acquired at 750 MHz using a Varian Unity 750 spectrometer at 277 K in the European Large Scale Facility at Utrecht University. The WATERGATE pulse sequence [33] was used for solvent suppression. All proton 2D spectra were acquired using the States-TPPI method for quadrature detection, with 2K × 512 complex data points and 16 scans per increment for 2D TOCSY and 64 scans for 2D NOESY experiments, respectively. The mixing time for TOCSY spectra was 80 ms. Mixing times for NOESY experiments were set to 100, 200, 350 and 400 ms to determine NOE build up rates. A mixing time of 350 ms provided sufficient cross-peak intensity without introducing spin-diffusion effects in the 2D NOESY. Phase-sensitive 2D NOESY was used for specific assignment and for estimation of proton–proton distance constrains. Data were zero filled in t_1 to give 2K × 2K real data points, and 90° phase-shifted square cosine–bell window function was applied in both dimensions. All spectra were processed by using NMRPipe software package [34] and analysed with NMRVIEW [35].

Interproton distances for AII were derived by measuring cross-peak intensities in the NOESY spectra. Intensities were calibrated to give a set of distance constraints using the NMRVIEW software package [35]. NOEs cross-peaks were separated into three distance categories according to their intensity. Strong NOEs were given an upper distance restraint of 3.0 Å, medium NOEs a value of 4.0 Å, and weak NOEs 5.5 Å. The lower distance limits were set to 1.8 Å.

A natural abundance ^{1}H-^{13}C HSQC NMR spectrum was acquired on a Bruker Avance 600 MHz spectrometer at 277 K in Utrecht. The spectrum was acquired with 2K × 400 points, with 48 scans per increment. The t_1 dimension was zero-filled to 1K, to give 1K × 1K real points, and 90° square cosine–bell window function was applied in both dimensions.

Structure calculations

All calculations were performed with CNS [36] using the ARIA setup and protocols [37,38], as described by Bonvin *et al.* [39]. Covalent interactions were calculated with the 5.2 version of the PARALLHDG parameter file [37,38] based on the CSDX parameter set [40]. Nonbonded interactions were calculated with the repel function using the PROLSQ parameters [41] as implemented in the new PARALLHDG parameter file. The OPLS nonbonded parameters [42] were used for the final water refinement including full van der Waals and electrostatic energy terms.

A simulated annealing protocol in Cartesian space was used starting from an extended conformation, and consisted of four stages: (a) high-temperature simulated annealing stage (10 000 steps, 2000 K); (b) a first cooling phase from 2000 to 1000 K in 5000 steps; (c) a second cooling phase from 1000 to 50 K in 2000 steps; finally (d) 200 steps of energy minimization. The time step for the integration was set to 0.003 ps.

Table 1. Summary of input restraint and structural statistics. Based on the 13 structures, obtained by simulated annealing in CNS followed by refinement in explicit water using NOE distance restraints, dihedral angle restraints, bond, angles, impropers, dihedral angle, van der waals and electrostatic energy terms.

RMSD (Å) with respect to mean	
Heavy backbone atoms (residues 1–8)	0.73 ± 0.23
All heavy atoms (residues 1–8)	1.35 ± 0.29
Number of experimental restraints	
Total NOEs	262
Intraresidue NOEs	87
Interresidue sequential NOEs ($\|i-j\| = 1$)	114
Interresidue medium-range NOEs ($1 < \|i-j\| < 4$)	59
Interresidue long-range NOEs ($\|i-j\| > 4$)	2
Restraint violations statistics	
NOE distances with violations > 0.3 (Å)	0
RMSD for experimental restraints (Å)	0.087 ± 0.005
CNS energies from SA[a,b]	
F_{vdw} (kcal·mol^{-1})	207 ± 37
F_{elec} (kcal·mol^{-1})	− 27 ± 4

[a] Force constants are described in Materials and methods. [b] The Lennard–Jones 3–7 and coulomb energy terms were calculated within CNS using the OPLS nonbonded parameters (as described in Materials and methods).

The structures were subjected to a final refinement protocol with explicit waters by solvating them with a 8 Å layer of TIP3P water molecules [42]. The resulting structures were energy minimized with 100 steps of Powell steepest descent minimization and the structure stereochemistry was evaluated through PROCHECK [43]. Restraint numbers and structural statistics for AII are presented in Table 1.

Results and discussion

High-resolution NMR structure of AII in aqueous solution

High-field NMR spectroscopy. The NMR experiments were performed at low temperature (277 K) to limit the conformational ensemble of the hormone in solution and to avoid unfavourable correlation times (i.e. when $\tau_c\omega_0 \cong 1$), which result in minimum NOE intensities. Resonance assignments were made using standard high-field 2D methods [44] and are given in Table S1 of the supplementary material. The primary NMR data used in structure calculations were interproton NOEs obtained from ^{1}H–^{1}H 2D NOESY experiments (Fig. 1). A list of NOEs, used for the structure calculations, is given in Table S2 of the supplementary material.

To investigate whether an amide proton is directly involved in intramolecular hydrogen bonding, the amide proton temperature coefficients ($\Delta\delta/\Delta T$) were measured. Exposed NHs typically have gradients in the range of −6.0 to −8.5 p.p.b./K, hydrogen-bonded or protected NHs apparently have $\Delta\delta/\Delta T$ of −2.0 to ±1.4 p.p.b.·K^{-1} [45]. For peptide fragments, however, because of conformational averaging $\Delta\delta/\Delta T$ values may lie between −28 and +12 p.p.b.·K^{-1}, resulting in a correlation between the gradient and structure that lies outside the rules mentioned above [45]. A plot of $\Delta\delta/\Delta T$ vs. the chemical shift deviation (CSD) of the measured amide proton resonances at 277 K (Fig. 2), with appropriate random coil chemical shift correction [46–48], provides a better correlation with partial structuring of a flexible linear peptide. The dashed line ($\Delta\delta/\Delta T = -7.8$ (CSD) −4.4) represents the cut off of $\Delta\delta/\Delta T$ between exposed and sequestered NHs of proteins. Gradients above the dashed line indicate exposed NHs, whereas those below indicate sequestered NHs. As can be seen in Fig. 2, all the backbone NH, with the exception of the Arg2, are above the dashed line, indicating that these peptide protons are somewhat exposed. The Arg2 backbone NH is most probably implicated in the formation of an intramolecular hydrogen bond (see discussion below). Low $\Delta\delta/\Delta T$ values for the backbone NH of Arg2 have been found in cyclic analogues of AII, suggesting shielding from the solvent, but with no rationalization about the structural origin of this effect [29].

$^1H^{\alpha}$, $^{13}C^{\alpha}$ and $^{13}C^{\beta}$ chemical shifts are known to be strongly dependent on the nature of protein/peptide secondary structure. Figure 3 shows a region of the natural abundance ^{1}H-^{13}C HSQC and the secondary shifts (deviation of the observed chemical shifts from the random coil chemical shift values [46,47] per residue of the amino-acid sequence of AII). The results are indicative, in a qualitative way, of a folded structure for the central fragment of AII. Interestingly, His6 illustrates the largest deviation of $^{13}C^{\alpha}$ chemical shifts from the random coil values. The origin of this phenomenon could be due to specific secondary features of the hormone affecting the observed chemical shifts (ring current, electric field, hydrogen-bond effects). ^{13}C-NMR resonance assignments and chemical shifts are given in Table S3 of the supplementary material.

$^3J_{HN\text{-}H\alpha}$ backbone-coupling constants were also extracted from the NMR spectra. This parameter tends to be small (< 6.0 Hz) in residues in a α-helical conformation and large (> 8.0 Hz) when extended; intermediate values (6–8 Hz) do not allow an unambiguous structural categorization [44]. For the Val3 and Ile6 residues, the $^3J_{HN\text{-}H\alpha}$ values are slightly bigger than 8 Hz (see Table S4 of the supplementary material), and are indicative of an extended conformation. For the residues Arg2, Tyr4, His6 and Phe8 in AII, this parameter is not structurally discriminatory between the two limiting cases. The intermediate values (6.4 Hz) of the backbone couplings for Tyr4 and His6 are possibly the result of twisting or bending in the middle of the amino-acid sequence of the hormone [49].

Structure calculations and analysis

The presence of conformational averaging in linear peptides can complicate the calculation of singular structures. In particular, the use of intraresidue and sequential NOEs, which are likely to have substantial contributions from folded and unfolded states, is problematic [50]. Two sets of structure calculations were implemented, considering: (a) sequential ($|i-j| = 1$), medium ($1 < |i-j| < 4$) and long-range ($|i-j| > 4$) NOE cross-peaks and (b) medium ($1 < |i-j| < 4$) and long-range ($|i-j| > 4$) NOE cross-peaks. The resulting conformational ensembles for cases (a)

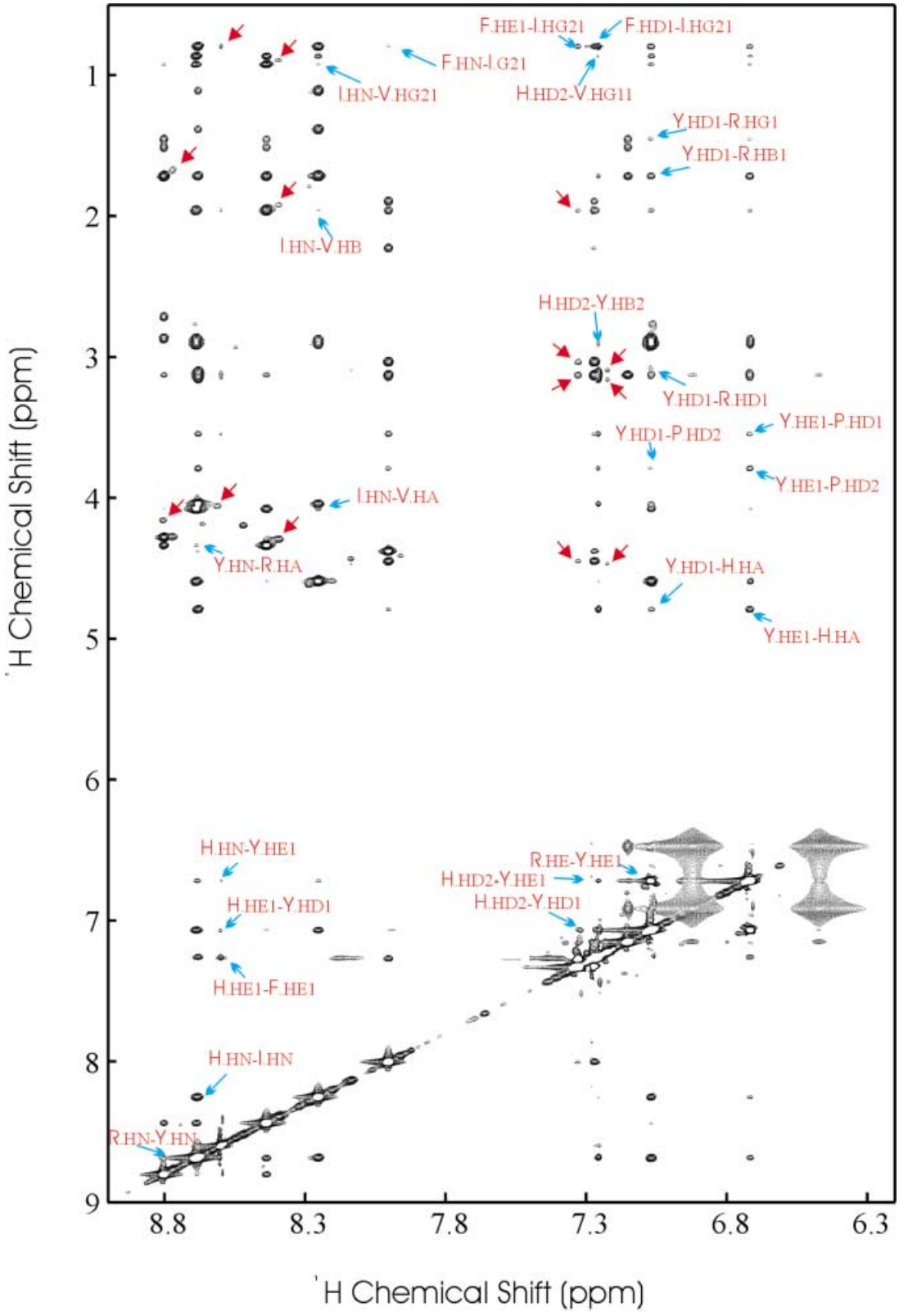

Fig. 1. Selected region of a 750-MHz NOESY spectrum (350 ms mixing time) of AII (90% H_2O/10% D_2O). Cross-peaks characteristic of the folded conformation are annotated. The red arrows denote the presence of the minor *cis* isomer.

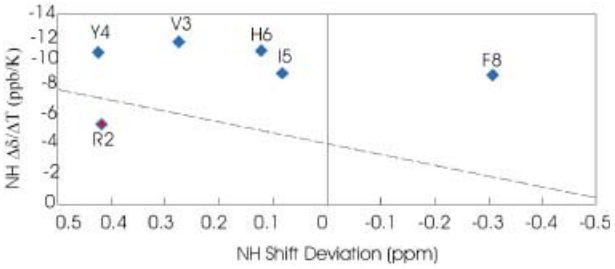

Fig. 2. NH Δδ/ΔT vs. CSD for AII in water solution and pH 5.7. The dashed line corresponds to $\Delta\delta/\Delta T = -7.8$ (CSD) −4.4, which provides the optimum differentiation of sequestered NHs in the protein database.

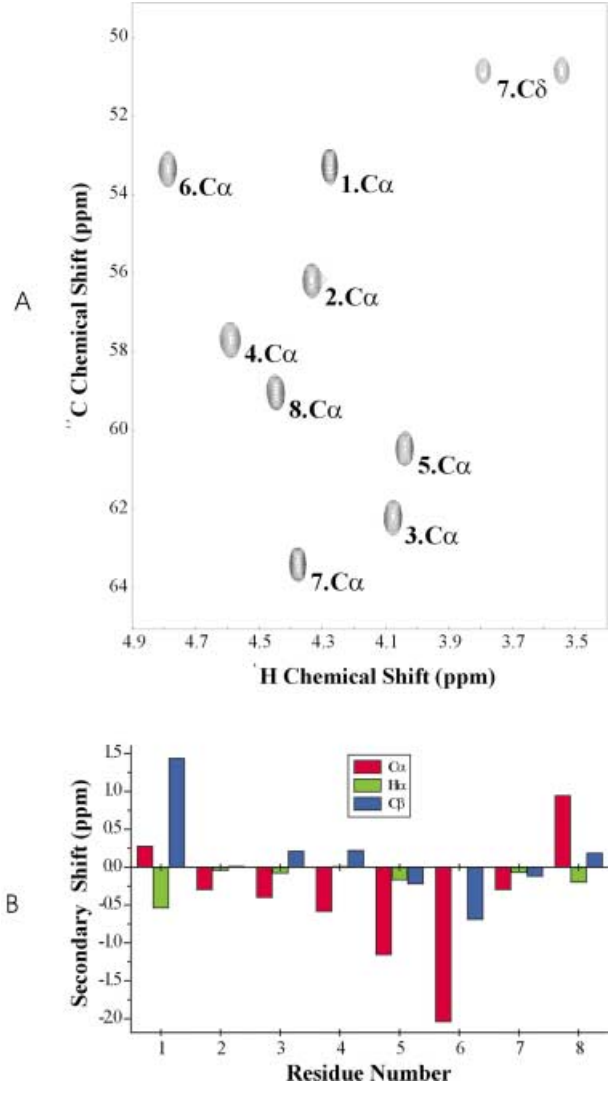

Fig. 3. (A) Selected region of a ^{1}H-^{13}C HSQC spectrum of AII and (B) secondary chemical shifts (deviation of the observed chemical shifts from the random coil chemical shift values) per residue of the amino-acid sequence of AII.

and (b) suggested the same overall fold and side chain orientation for the hormone. In addition, we checked for the presence of conformational averaging by performing ensemble-average refinement with complete cross-validation against the number of conformers [51,52]. This procedure indicated that a single conformer was sufficient to satisfy the experimental restraints (Figure S1 of the supplementary material).

In the second set of calculations, 173 sequential and medium range NOEs and two long-range NOEs were used as distance restraints for AII (Table S2 of the supplementary material). No explicit dihedral or hydrogen-bonding restraints were applied. Structure calculations were performed using a simulated annealing protocol, following ARIA/CNS setup [36–40]. A family of 200 structures was calculated. Forty-eight structures with the lowest energy and NOE violations of no larger than 0.25 Å were selected after the final refinement in explicit water. The conformation of the hormone does not change significantly in the final stages of refinement and is mainly determined by the NMR data. The quality of the structures, however, improved after water refinement because both electrostatic and full Lennard-Jones potentials are used. From the family of the 48 structures, 13 structures were selected having the best allowed regions in the Ramachandran plot (Fig. 4). The RMSD value of the ensemble of the 13 calculated structures, with respect to mean structure, for backbone atoms (residues 1–8) was found to be 0.73 ± 0.23 Å and for all heavy atoms 1.35 ± 0.29 Å (Table 1).

The most well-defined fragment of the peptide hormone contains the amino-acid residues 3–7. Figure 5A (a,b) provides a superposition of backbone and heavy atom of the entire ensemble of the 13 calculated structures for the 3–7 fragment. Figure 5B (a) illustrates a representative conformer whose structure is the closest to the average co-ordinates of the ensemble.

The structures calculated from NMR-derived restraints have a well-defined U-shaped conformation for the backbone with a *trans* His-Pro amide bond. The RMSD values for the backbone C^{α}, N, C′ atoms from the mean structure for the 3–7 fragment is 0.14 ± 0.05 Å and for all the heavy atoms (C^{α}, N, C′, O) the RMSD is 0.32 ± 0.15 Å. The RMSD values of the backbone atoms from the mean value for the 4–7 fragment is 0.10 ± 0.04 Å and for all heavy atoms the RMSD is 0.32 ± 0.16 Å. The N-terminal and C-terminal tails are less well defined by the available restraints.

The present NMR study clearly demonstrates that in aqueous solution, even small peptide hormones can adopt favoured, rather well defined conformations. Thus, in aqueous solution, AII adopts a fairly compact structure with its C-termini and N-termini approaching to within ≈ 7.2 Å of each other. Furthermore, the side chains of Arg2, Tyr4, Ile5, His6 are oriented on one side of a plane defined by the peptide backbone, and the Val3 and Pro7 are pointed to opposite directions. The Tyr4 side chain is oriented inside the folded conformation of the molecule, and Arg2 is exposed to the solvent, as illustrated in Fig. 5B,a. The stabilization of the folded conformation can be explained by the stacking of the Val3 side chain with the Pro7 ring (this is consistent with the observed long-range NOE cross-peaks and the distance between, e.g. Val3 C^{γ} and Pro7 C^{γ} which is

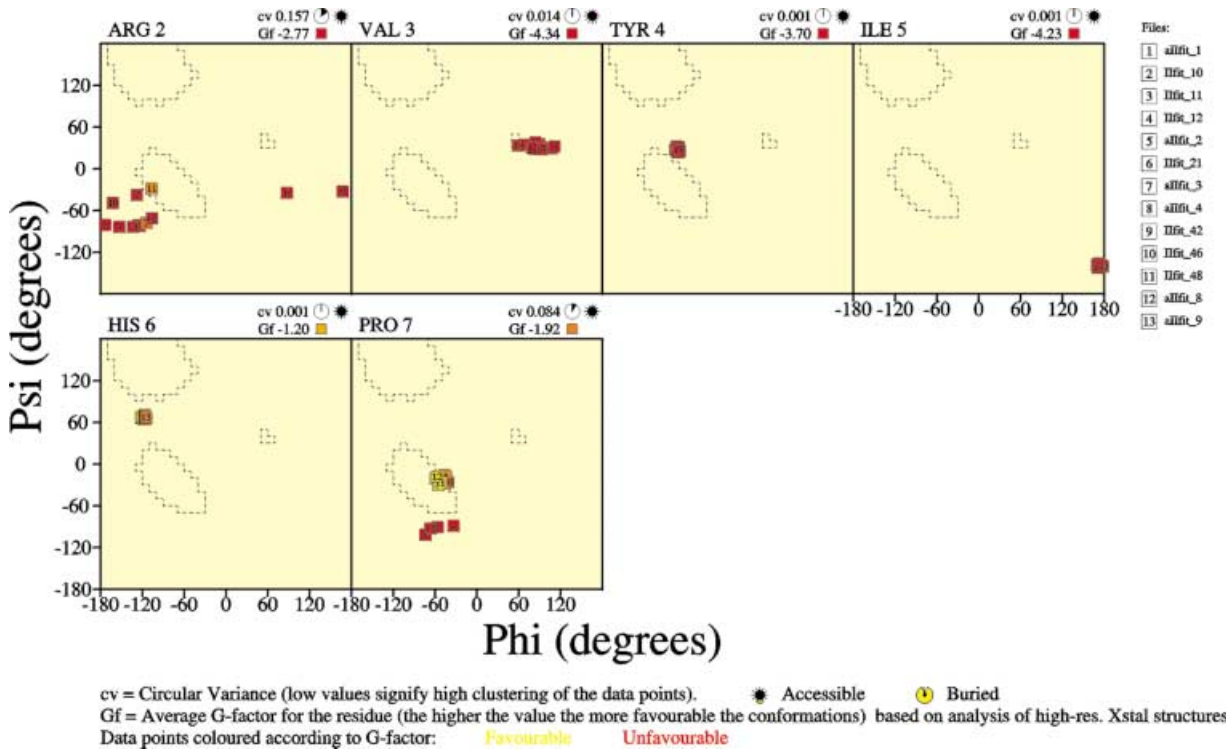

Fig. 4. Ensemble Ramachandran plots of the 13 solution structures of AII.

≈ 3.2 Å) and by a hydrophobic cluster formed by the Tyr4, Ile5 and His6 side chains (Fig. 6). Analysis of the distance between the N-terminus and C-terminus of the peptide for the individual conformers indicates that the compact conformation of the octapeptide is not stabilized by a salt bridge between the two charged groups.

It is interesting to compare the overall fold of AII from the present study with previously reported conformations for AII in solution. An 'open turn' conformation for the Tyr4-Ile5 residues has been observed with NMR by Nikiforovich *et al.* [29] in cyclic AII analogues, containing a disulfide bridge between positions 3 and 5. Detailed conformation–biological activity studies of Fermandjian *et al.* [53] in a series of AII analogues substituted in Ile5, confirmed the steric influence of residue 5 on the organization of Tyr4 and His6 side chains. In addition, structure–activity relationship studies highlighted the requirement of a lipophilic and β-branched hydrocarbon moiety in the fifth position for high pressor activity of AII analogues [54]. In accordance with our model, this could be explained through the formation of a hydrophobic cluster by the Tyr4, Ile5 and His6 side chains, as illustrated in Fig. 6B.

Recently, NMR studies of AII in a phospholipid micelle solution were interpreted in terms of a well-defined hairpin compact structure, similar to our aqueous solution structure, with the N-terminus and C-terminus approaching to within 7.6 Å of each other [23] and an inverse γ-turn encompassing residues His6, Pro7 and Phe8. The Tyr4, His6 and Phe8 side chains were found to be close together in space. The orientation of the Tyr4 side chain is similar in the two structures, with a dihedral (χ_1) angle 65(8)° in the phospholipid environment and 46.5 (5.1)° in aqueous solution. The Asp1 side chain carboxylic group was suggested to be involved in hydrogen-bonding interaction with either the N-terminal amino group or the Arg2 side chain amino group, whereas in our studies a hydrogen bond is formed with the backbone NH of Arg2. Similar investigations in conformationally restrictive environment (DodChoP micelles) [15], by the use of ultraviolet resonance Raman and absorption studies, provided evidence that AII adopts a folded turn-like structure and that Tyr4 is either involved in a hydrogen bond through its hydroxy group or it is buried in a hydrophobic milieu. The latter seems to be a more plausible explanation in the frame of the observed hydrophobic cluster in our study.

In conclusion, the similarity of the folded structure of AII in aqueous solution and in conformationally restrictive phospholipid environment clearly demonstrates that the presence of a hydrophobic–hydrophilic interface does not play a determinative role in conferring the structure of AII.

X-ray structure of AII bound to the mAb Fab131: comparison with the NMR solution structure

The phenomenon of conformational stabilization [55] and selection between different antigen conformers has been demonstrated by means of antibodies that act on a population of antigen molecules with different extents of conformational order [56,57]. Thus, a 'surrogate system' that consists of a high-affinity monoclonal antibody (mAb131) and AII had been used to study a bound conformation of AII [30]. The 3D structure of the AII–Fab complex has been refined by Garcia *et al.* [30]. The binding site of the antibody is very deep and narrow. This has two effects: (a) it markedly increases the exposed surface area of the free mAb; (b) it creates space from which it is easy to

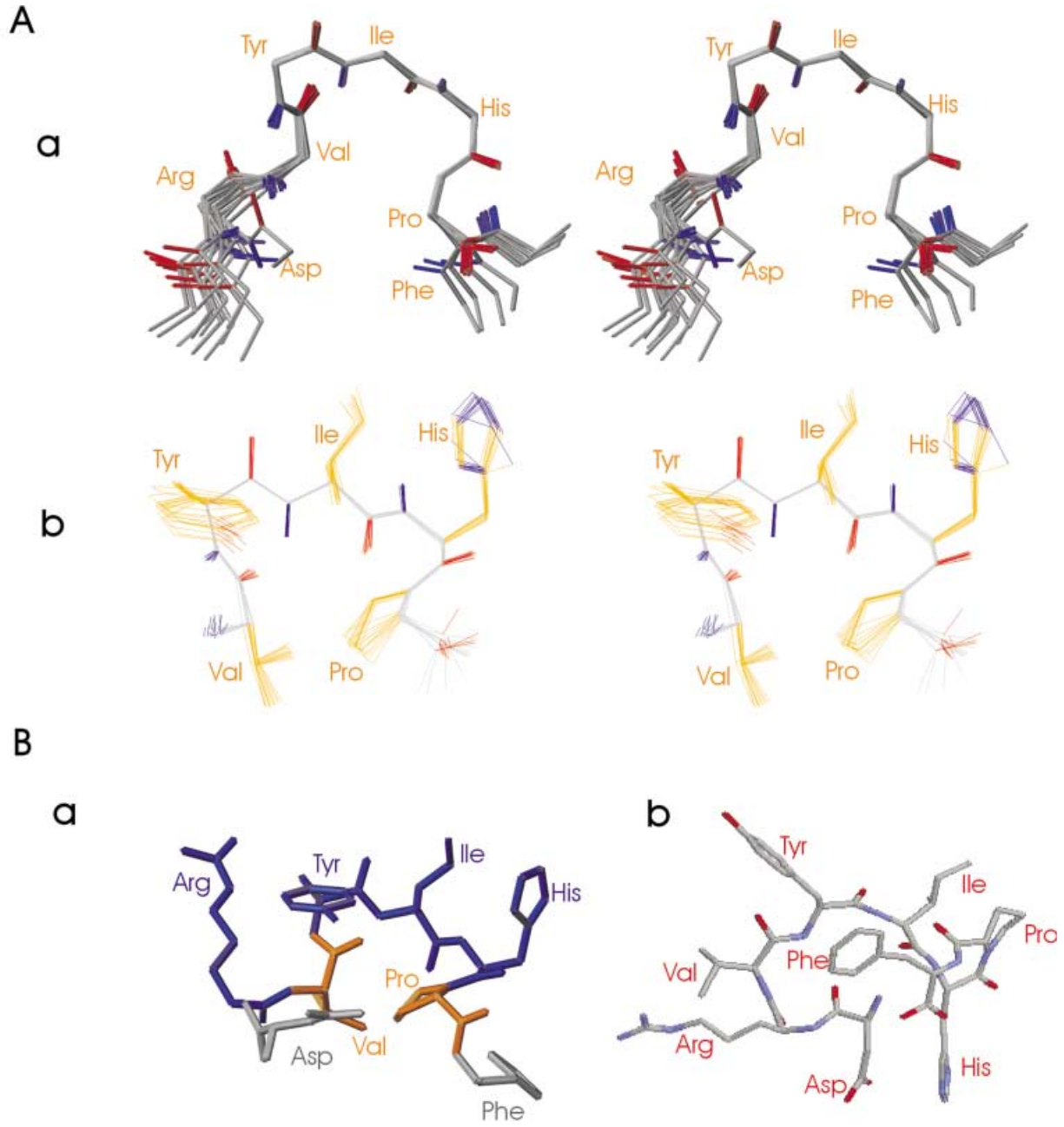

Fig. 5. Structure of AII. (A) Solution conformation of AII. (a) The 13 structures calculated for AII overlaid using the N, C^{α} and C′ atoms of residues 3–7. (b) Superposition of the backbone and heavy atoms of the fragment 3–7 of AII. (B) Comparison of a representative conformer of AII with structure closest to the average co-ordinates (the blue colour denotes the side chains of Arg2, Tyr4, Ile5, His6 and the yellow the side chains of Val3 and Pro7) (a) with the the X-ray structure of AII in the Fab131–AII complex [30] (b).

exclude solvent by filling the cavity. The most buried residues of AII are of the central AII sequence Tyr4-Ile5-His6-Pro7, which is also the most immunogenic epitope of the peptide [58–60]. Most substitutions of these immunogenic residues abolish binding to both mAb131 and AT_1.

The AII bound to the mAb adopts a compact conformation with two turns (Fig. 5B,b). The first turn involves residues Asp1 and Arg2 and brings the N-terminus of the peptide in spatial proximity to the C-terminus of the peptide. It was suggested that the stabilization of such a tight conformation may result from the formation of a salt bridge between the termini and a hydrogen bond between the $-NH_3^+$ terminal of Asp1 and the main chain carbonyl group of Ile5 [30]. The second turn involves the residues Ile5, His6, Pro7, and the centre of this turn is lodged in the deepest region of the binding site. This tight VIb-type turn contains a *cis* His6-Pro7 peptide bond ($\omega \approx 40^{\circ}$) which results in a 90° twist of this part of the backbone with respect to the rest of the molecule. Evidence for the presence of a highly populated VIb turn-like conformation was also

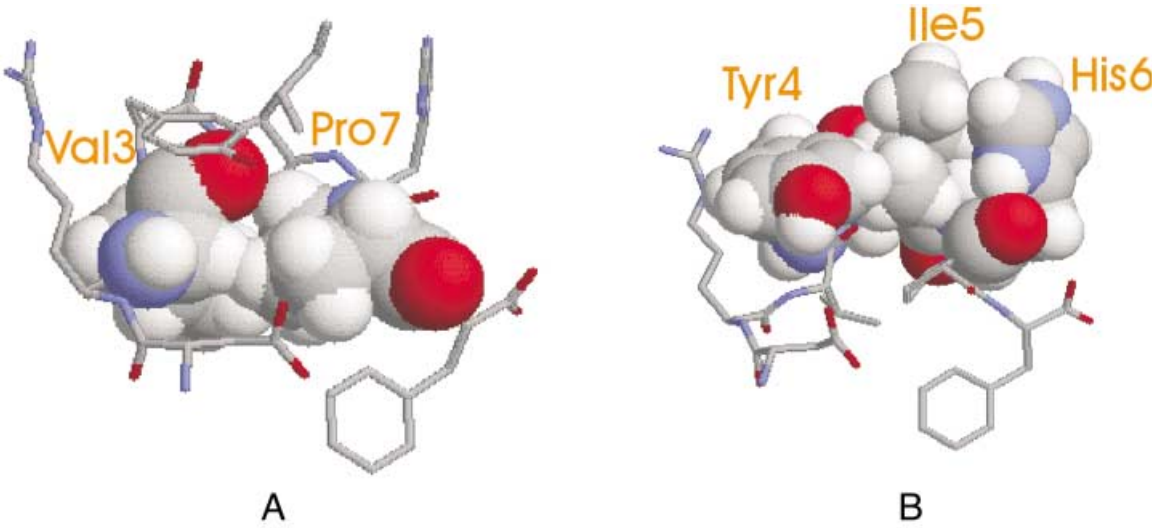

Fig. 6. Structure of a representative folded conformer of AII showing the van der Waals contacts between the side-chains of residues Val3 and Pro7 (A) and Tyr4, Ile5, and His6 (B). Carbon atoms are shown in grey, oxygen atoms in red, nitrogen atoms in blue, and hydrogen atoms in white.

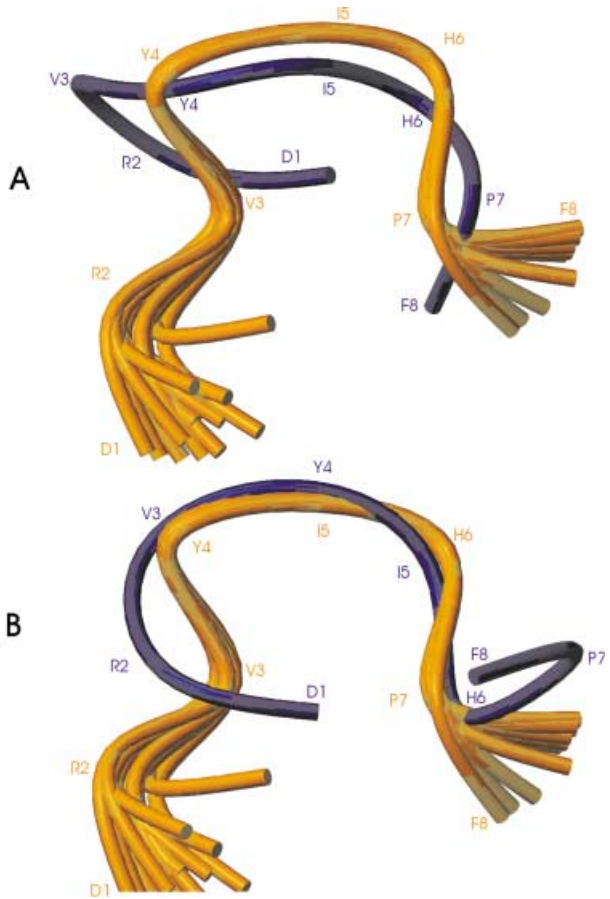

Fig. 7. (A) Sequence alignment of the fragment 4–7 of the backbone of the 13 ensemble solution structures of AII (brown colour) superimposed on the X-ray structure (dark blue colour) and (B) structure alignment of the fragment 4–7 of the 13 ensemble structures of AII to the fragment 3–6 of the X-ray structure of AII.

provided for the *cis* X-Pro isomers of several peptides with the sequence motif X-Pro-Phe [61] (X stands for aromatic amino acid). This specific conformational feature may be of importance for the conformation of the AII complexed to the AT_1 G-protein-coupled receptor and the activation of the receptor. Interestingly, a *cis* to *trans* conformational switch isomerization of the 11-*cis*-retinal chromophore of rhodopsin is of primary importance for stimulation of the receptor and transformation to the signalling state [62].

The present NMR data provide the basis for a quantitative comparison of the structure of AII in solution with the X-ray structure of AII complexed to the Fab131 mAb. In Fig. 7A, a sequence alignment is represented of the backbone of the conformational ensemble of AII in solution state with the backbone of the X-ray structure. In Fig. 7B, the models are superimposed using structural alignments only. Table 2 illustrates the RMSD values obtained after the sequence and structure alignment of the two structures by using the program Profit1.8. Remarkably, the superposition of the solution state and the bound structure of AII exhibits small RMSD positional differences between the two structures.

Table 2. Average backbone atomic root mean square positional differences between the X-ray structure of AII and the ensemble of 13 AII calculated structures. Superposition is based on sequence and structure alignment.

Residue number range in the X-ray structure of AII	Residue number range in the solution average structure of AII	Backbone (C′, N, C^{α}) RMSD (Å)
2–7	2–7	1.99 ± 0.04
3–7	3–7	1.90 ± 0.04
3–6	3–6	1.30 ± 0.03
4–7	4–7	1.27 ± 0.02
2–5	3–6	0.82 ± 0.03
2–6	3–7	1.07 ± 0.05
3–6	4–7	0.76 ± 0.03

Thus, it can be concluded that small rearrangements of the backbone on binding are required by a mean value of about 1.27 ± 0.02 Å for sequence alignment and 0.76 ± 0.03 Å for structure alignment of the most immunogenic epitope 4–7 of AII. This part of the peptide hormone therefore is quite rigid and prearranged in the solution state for binding at the receptor–antigen recognition site.

The common features among the solution structure of AII and the bound conformation to the antibody Fab131 are:

(a) the first turn (Asp1 and Arg2) which induces the orientation of the N-terminal part to the C-terminal part of the molecule;
(b) the second turn (His6, Pro7, Phe8);
(c) the third turn (Ile5, His6 and Pro7).

The crystallographic distance of the Asp1 side chain (OD1) to the main chain NH of the proceeding Arg2 is ≈ 2.9 Å, underlying the possibility of the formation of a side chain–main chain hydrogen bond. This distance is comparable to that obtained from the NMR structure in solution (≈ 2.8 Å) and consistent with the measured NH temperature coefficients, which revealed the possible involvement of the Arg2 backbone NH proton in intramolecular hydrogen bonding. The experimental data of this study therefore demonstrate the formation of an Asx-like turn with the side chain carbonyl group of aspartate hydrogen-bonded to the main chain NH of the preceding arginine, forming a stable heptamer ring, both in the X-ray structure and the solution structure of AII (Fig. 8). Indeed, aspartate residues at the N-termini of short polypeptides have shown a stabilizing influence [63,64]. These effects are thought to result from an interaction of the negative charge with the dipole of the polypeptide chain. Examination by Wan and Milner-White [65] of several high-resolution crystal structures of the ways that side chain carboxylates form hydrogen bonds with main chain atoms revealed a high incidence of Asx motifs with the aspartate or asparagine as the first residue. Specifically Asx motifs occur with the side chain aspartate carboxyl group hydrogen-bonded to a main chain NH group of the residue two to three amino acids ahead.

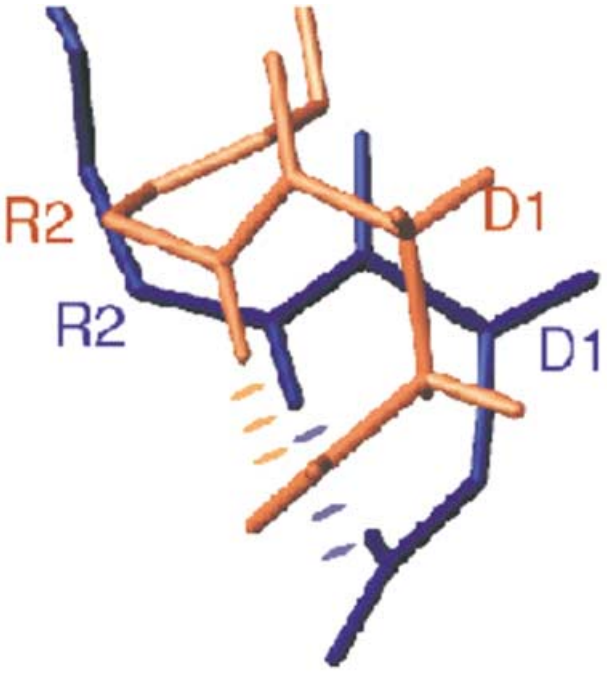

Fig. 8. The Asx-like motif of AII in the NMR structure (brown colour) and in the X-ray structure (blue colour). The hydrogen bond is shown by the dashed line.

Several structure–activity studies of AII have delineated the requirements for agonist activity, highlighting Tyr4 and Phe8 as basic requirements for high pressor activity of AII; substitution with other amino acids results in antagonistic analogues. Furthermore, Tyr4 has been suggested to be a switch residue responsible for receptor activation. Specifically, it has been proposed that the activation of the AT_1 receptor from the basal state requires a key interaction between Asn111, in the transmembrane helix III (TM3) of the receptor, and the Tyr4 of AII [66,67]. Interestingly, the side chain of Tyr4 of the free hormone in aqueous solution adopts a very low RMSD value, and it is oriented inside the overall fold of the molecule, whereas in its bound state it is oriented outside the fold towards the receptor site. Very probably, this ≈ 130° rearrangement in the χ_1 angle requires a small energy conformational barrier for the initial step of the receptor–peptide recognition and could be responsible for initiating a biochemical cascade upon the interaction of Tyr4 with Asn111 [68].

Constructively, the overall fold of AII in aqueous solution state is reminiscent of the conformation observed when AII is bound to the mAb Fab131. However, in the crystal structure of the complex, a hydrogen bond between the -NH_3^+ terminal of Asp1 and the main chain carbonyl group of Ile5 is observed, which is not the case in aqueous solution. In the X-ray structure, AII has a *cis* His-Pro amide bond. In our NMR spectra of AII in solution, we do observe additional peaks that can be attributed to a minor population of less than 10% with the His-Pro bond in the *cis* conformation (Fig. 1). The presence of such a conformation in the crystal complex (with $\omega \approx 40^{\circ}$) and its low fraction in aqueous solution indicate that it is energetically strained, and that the extensive intermolecular interactions observed in the complex are necessary to compensate for the free strain. For example, there are several close contacts of His6 and Pro7 of AII to Ser^{L91}, Tyr^{L95}, Arg^{H52} and Tyr^{L92}, Ala^{H33}, Arg^{H52} and Arg^{H99}, respectively, in the Fab131 'receptor' site [30].

The results obtained in our studies suggest that the folded conformation of AII in aqueous solution is optimal for receptor–antigen recognition, and that binding and the energetic cost of deforming it into the bound conformation is compensated by the energetic benefit that could be obtained from intermolecular contacts in the bound state. We argue therefore that pre-existing subpopulations of ligand–peptide conformers preferentially bind to their corresponding receptor in a frame of 'complementarity'. As pointed out by Porschke and Eigen [69], a mechanism for information transfer must satisfy the dual criteria of selectivity and speed. High selectivity is most rapidly achieved by having a relatively large recognition site (pointing out common structural features among free and bound ligand). Conformational studies therefore of small

peptide hormones, such as AII, in aqueous solution may have important consequences in delineating structure–function relationships and the principles of biomolecular hormone–receptor interaction and recognition. Further work along these lines is currently underway in our laboratories.

Acknowledgements

A.G.T. acknowledges the Federation of European Biochemical Societies (FEBS) for a summer fellowship. The 750 and 600 MHz spectra were recorded at the SONNMR Large Scale Facility in Utrecht, which is funded by the 'Access to Research Infrastructures Programm of the European Union' (HPR1-CT-1999-00005). We also thank the SON-NMR Large Scale Facility for the use of the computational facilities.

References

1. Samanen, J. & Regoli, D. (1994) Structure–activity relationships of peptide angiotensin II receptor agonists and antagonists. In *Angiotensin II Receptors* (Ruffdo, R.R., ed.), Vol. 2, pp. 11–97. CRC Press, Boca Raton, FL.
2. Ji, T.H., Grossmann, M. & Ji, I.H. (1998) G protein-coupled receptors I. Diversity of receptor–ligand interactions. *J. Biol. Chem.* **273**, 17299–17302.
3. Timmermans, P.B., Wong, P.C., Chiu, A.T., Herblin, W.F., Benfield, P., Carini, D.J., Lee, R.J., Wexler, R.R., Saye, J.A. & Smith, R.D. (1993) Angiotensin II receptors and angiotensin II receptor antagonists. *Pharmacol. Rev.* **45**, 205–251.
4. Pellegrini, M. & Mierke, D.F. (1999) Structural characterization of peptide hormone/receptor interactions by NMR spectroscopy. *Biopolymers* **51**, 208–220.
5. Strader, C.D., Fong, T.M., Tota, M.R., Underwood, D. & Dixon, R.A. (1994) Structure and function of G protein-coupled receptors. *Annu. Rev. Biochem.* **63**, 101–132.
6. Kuhlbrandt, W. & Gouaux, E. (1999) Membrane proteins. *Curr. Opin. Struct. Biol.* **9**, 445–447.
7. Burgen, A.S., Roberts, G.C. & Feeney, J. (1975) Binding of flexible ligands to macromolecules. *Nature (London)* **253**, 753–755.
8. Loosli, H.R., Kessler, H., Oschkinat, H., Weber, H.P., Petcher, T.J. & Widmer, A. (1985) Peptide conformations. 31. The conformation of cyclosporin-A in the crystal and in solution. *Helv. Chim. Acta* **68**, 682–704.
9. Vanduyne, G.D., Standaert, R.F., Karplus, P.A., Schreiber, S.L. & Clardy, J. (1991) Atomic-structure of Fkbp-Fk506, an immunophilin-immunosuppressant complex. *Science* **252**, 839–842.
10. Michnick, S.W., Rosen, M.K., Wandless, T.J., Karplus, M. & Schreiber, S.L. (1991) Solution structure of Fkbp, a rotamase enzyme and receptor for Fk506 and rapamycin. *Science* **252**, 836–839.
11. Wüthrich, K., Vonfreyberg, B., Weber, C., Wider, G., Traber, R., Widmer, H. & Braun, W. (1991) Receptor-induced conformation change of the immunosuppressant cyclosporin-A. *Science* **254**, 953–954.
12. Moroder, L., Romano, R., Guba, W., Mierke, D.F., Kessler, H., Delporte, C., Winand, J. & Christophe, J. (1993) New evidence for a membrane-bound pathway in hormone receptor binding. *Biochemistry* **32**, 13551–13559.
13. Smeby, R.R., Arkawa, K., Bumpus, F.M. & Marsh, M.M. (1962) A proposed conformation of isoleucine^5–angiotensin II. *Biochim. Biophys. Acta* **58**, 550–557.
14. Printz, M.P., Williams, H.P. & Craig, L.C. (1972) Evidence for the presence of hydrogen-bonded secondary structure in angiotensin II in aqueous solution. *Proc. Natl Acad. Sci. USA* **69**, 378–382.
15. Cho, N.J. & Asher, S.A. (1996) UV resonance Raman and absorption studies of angiotensin II conformation in lipid environments. *Biospectroscopy* **2**, 71–82.
16. Nikiforovich, G.V., Vesterman, B.G. & Betins, J. (1988) Combined use of spectroscopic and energy calculation methods for the determination of peptide conformation in solution. *Biophys. Chem.* **31**, 101–106.
17. Greff, D., Fermandjian, S., Fromageot, P., Khosla, M.C., Smeby, R.R. & Bumpus, F.M. (1976) Circular-dichroism spectra of truncated and other analogs of angiotensin II. *Eur. J. Biochem.* **61**, 297–305.
18. Fermandjian, S., Morgat, J.L. & Fromageot, P. (1971) Studies of angiotensin-II conformations by circular dichroism. *Eur. J. Biochem.* **24**, 252–258.
19. Printz, M.P., Nemethy, G. & Bleich, H. (1972) Proposed models for angiotensin II in aqueous solution and conclusions about receptor topography. *Nat. New Biol.* **237**, 135–140.
20. Fermandjian, S., Fromageot, P., Tistchenko, A.M., Leicknam, J.P. & Lutz, M. (1972) Angiotensin II conformations. Infrared and Raman studies. *Eur. J. Biochem.* **28**, 174–182.
21. Paiva, T.B., Paiva, A.C.M. & Scheraga, H.A. (1963) The conformation of angiotensin II in aqueous solution. *Biochemistry* **2**, 1327–1334.
22. Cushman, J.A., Mishra, P.K., Bothner-By, A.A. & Khosla, M.S. (1992) Conformations in solution of angiotensin II, and its 1–7 and 1–6 fragments. *Biopolymers* **32**, 1163–1171.
23. Carpenter, K.A., Wilkes, B.C. & Schiller, P.W. (1998) The octapeptide angiotensin II adopts a well-defined structure in a phospholipid environment. *Eur. J. Biochem.* **251**, 448–453.
24. Matsoukas, J.M., Hondrelis, J., Keramida, M., Mavromoustakos, T., Makriyannis, A., Yamdagni, R., Wu, Q. & Moore, G.J. (1994) Role of the NH_2-terminal domain of angiotensin II (ANG II) and [Sar1]angiotensin II on conformation and activity. NMR evidence for aromatic ring clustering and peptide backbone folding compared with [des-1,2,3]angiotensin II. *J. Biol. Chem.* **269**, 5303–5312.
25. Weinkam, R.J. & Jorgensen, E.C. (1971) Angiotensin II analogs. IX. Conformational studies of angiotensin II by proton magnetic resonance. *J. Am. Chem. Soc.* **93**, 7038–7044.
26. Kataoka, T., Beusen, D.D., Clark, J.D., Yodo, M. & Marshall, G.R. (1992) The utility of side-chain cyclization in determining the receptor-bound conformation of peptides: cyclic tripeptides and angiotensin-II. *Biopolymers* **32**, 1519–1533.
27. Bleich, H.E., Galardy, R.E., Printz, M.P. & Craig, L.C. (1973) Conformational studies of angiotensin peptides in aqueous solution by proton magnetic resonance. *Biochemistry* **12**, 4950–4957.
28. Bleich, H.E., Galardy, R.E. & Printz, M.P. (1973) Conformation of angiotensin II in aqueous solution. Evidence for the turn model. *J. Am. Chem. Soc.* **95**, 2041–2042.
29. Nikiforovich, G.V., Kao, J.L.F., Plucinska, K., Zhang, W.J. & Marshall, G.R. (1994) Conformational-analysis of 2 cyclic analogs of angiotensin: implications for the biologically-active conformation. *Biochemistry* **33**, 3591–3598.
30. Garcia, K.C., Ronco, P.M., Verroust, P.J., Brunger, A.T. & Amzel, L.M. (1992) Three-dimensional structure of an angiotensin II-Fab complex at 3 Å: hormone recognition by an anti-idiotypic antibody. *Science* **257**, 502–507.
31. Carpino, L.A. & Han, G.Y. (1972) The 9-fluorenylmethoxycarbonyl amino-protecting group. *J. Org. Chem.* **37**, 3404–3409.
32. Sarantakis, D., Teichman, J., Lien, E.L. & Fenichel, R.L. (1976) A novel cyclic undercapeptide, WY-40, 770, with prolonged growth hormone release inhibiting activity. *Biochem. Biophys. Res. Commun.* **73**, 366–342.

33. Piotto, M., Saudek, V. & Sklenar, V. (1992) Gradient-tailored excitation for single-quantum NMR spectroscopy of aqueous solutions. *J. Biomol. NMR* **2**, 661–665.
34. Delaglio, F., Grzesiek, S., Vuister, G.W., Zhu, G., Pfeifer, J. & Bax, A. (1995) NMRPipe: a multidimensional spectral processing system based on UNIX pipes. *J. Biomol. NMR* **6**, 277–293.
35. Johnson, B.A. & Blevins, R.A. (1994) NMR view: a computer-program for the visualization and analysis of nmr data. *J. Biomol. NMR* **4**, 603–614.
36. Brunger, A.T., Adams, P.D., Clore, G.M., DeLano, W.L., Gros, P., Grosse-Kunstleve, R.W., Jiang, J.S., Kuszewski, J., Nilges, M., Pannu, N.S., Read, R.J., Rice, L.M., Simonson, T. & Warren, G.L. (1998) Crystallography & NMR system: a new software suite for macromolecular structure determination. *Acta Crystallogr. Sect. D: Biol. Crystallogr.* **54**, 905–921.
37. Linge, J.P. & Nilges, M. (1999) Influence of non-bonded parameters on the quality of NMR structures: a new force field for NMR structure calculation. *J. Biomol. NMR* **13**, 51–59.
38. Nilges, M. & O'Donoghue, S.I. (1998) Ambiguous NOEs and automated NOE assignment. *Prog. Nucl. Magn. Reson. Spectrosc.* **32**, 107–139.
39. Bonvin, A., Houben, K., Guenneugues, M., Kaptein, R. & Boelens, R. (2001) Rapid protein fold determination using secondary chemical shifts and cross-hydrogen bond ^{15}N-$^{13}C'$ scalar couplings ($^{3hb}JNC'$). *J. Biomol. NMR* **21**, 221–233.
40. Engh, R.A. & Huber, R. (1991) Accurate bond and angle parameters for X-ray protein-structure refinement. *Acta Crystallogr. Section A: Found. Crystallogr.* **47**, 392–400.
41. Hendrickson, W.A. (1985) Stereochemically restrained refinement of macromolecular structures. *Methods Enzymol.* **115**, 252–270.
42. Jorgensen, W.L. & Tirado-Rives, J. (1988) The OPLS force field for proteins. Energy minimizations for crystals of cyclic peptides and crambin. *J. Am. Chem. Soc.* **110**, 1657–1666.
43. Laskowski, R.A., Macarthur, M.W., Moss, D.S. & Thornton, J.M. (1993) Procheck: a program to check the stereochemical quality of protein structures. *J. Appl. Crystallogr.* **26**, 283–291.
44. Wüthrich, K. (1986) *NMR of Proteins and Nucleic Acids*. John Wiley and Sons, New York.
45. Andersen, N.H., Neidigh, J.W., Harris, S.M., Lee, G.M., Liu, Z.H. & Tong, H. (1997) Extracting information from the temperature gradients of polypeptide NH chemical shifts. 1. The importance of conformational averaging. *J. Am. Chem. Soc.* **119**, 8547–8561.
46. Wishart, D.S., Bigam, C.G., Holm, A., Hodges, R.S. & Sykes, B.D. (1995) ^{1}H, ^{13}C and ^{15}N random coil NMR chemical shifts of the common amino acids. I. Investigations of nearest-neighbor effects. *J. Biomol. NMR* **5**, 67–81.
47. Schwarzinger, S., Kroon, G.J.A., Foss, T.R., Wright, P.E. & Dyson, H.J. (2000) Random coil chemical shifts in acidic 8 M urea: implementation of random coil shift data in NMRView. *J. Biomol. NMR* **18**, 43–48.
48. Wishart, D.S. & Sykes, B.D. (1994) The ^{13}C chemical-shift index: a simple method for the identification of protein secondary structure using ^{13}C chemical-shift data. *J. Biomol. NMR* **4**, 171–180.
49. Cochran, A.G., Tong, R.T., Starovasnik, M.A., Park, E.J., McDowell, R.S., Theaker, J.E. & Skelton, N.J. (2001) A minimal peptide scaffold for beta-turn display: optimizing a strand position in disulfide-cyclized beta-hairpins. *J. Am. Chem. Soc.* **123**, 625–632.
50. de Alba, E., Jimenez, M.A. & Rico, M. (1997) Turn residue sequence determines β-hairpin conformation in designed peptides. *J. Am. Chem. Soc.* **119**, 175–183.
51. Bonvin, A.M. & Brunger, A.T. (1995) Conformational variability of solution nuclear magnetic resonance structures. *J. Mol. Biol.* **250**, 80–93.
52. Bonvin, A.M. & Brunger, A.T. (1996) Do NOE distances contain enough information to assess the relative populations of multi-conformer structures? *J. Biomol. NMR* **7**, 72–76.
53. Fermandjian, S., Sakarellos, C., Piriou, F., Juy, M., Toma, F., Thanh, H.L., Lintner, K., Khosla, M.C., Smeby, R.R. & Bumpus, F.M. (1983) The key role of residue 5 in angiotensin II. *Biopolymers* **22**, 227–231.
54. Samanen, J., Narindray, D., Cash, T., Brandeis, E., Adams, W. Jr, Yellin, T., Eggleston, D., DeBrosse, C. & Regoli, D. (1989) Potent angiotensin II antagonists with non-beta-branched amino acids in position 5. *J. Med. Chem.* **32**, 466–472.
55. Rizzo, P., Tinello, C., Punturieri, A. & Taniuchi, H. (1992) A study of hydrogen exchange of monoclonal antibodies: specificity of the antigen-binding induced conformational stabilization. *Biochim. Biophys. Acta* **1159**, 169–178.
56. Berger, C., Weber-Bornhauser, S., Eggenberger, J., Hanes, J., Pluckthun, A. & Bosshard, H.R. (1999) Antigen recognition by conformational selection. *FEBS Lett.* **450**, 149–153.
57. Murphy, K.P., Xie, D., Garcia, K.C., Amzel, L.M. & Freire, E. (1993) Structural energetics of peptide recognition: angiotensin II/antibody binding. *Proteins* **15**, 113–120.
58. Couraud, P.O. (1987) Anti-angiotensin II anti-idiotypic antibodies bind to angiotensin II receptor. *J. Immunol.* **138**, 1164–1168.
59. Budisavljevic, M., Geniteau-Legendre, M., Baudouin, B., Pontillon, F., Verroust, P.J. & Ronco, P.M. (1988) Angiotensin II (AII)-related idiotypic network. II. Heterogeneity and fine specificity of AII internal images analyzed with monoclonal antibodies. *J. Immunol.* **140**, 3059–3065.
60. Budisavljevic, M., Ronco, P.M. & Verroust, P.J. (1990) Angiotensin II (AII)-related idiotypic network. III. Comparative analysis of idiotopes and paratopes borne by monoclonal antibodies raised against AII (AB1) and its internal image (AB3). *J. Immunol.* **145**, 1440–1449.
61. Yao, J., Dyson, H.J. & Wright, P.E. (1994) 3-dimensional structure of a type-VI turn in a linear peptide in water solution: evidence for stacking of aromatic rings as a major stabilizing factor. *J. Mol. Biol.* **243**, 754–766.
62. Teller, D.C., Okada, T., Behnke, C.A., Palczewski, K. & Stenkamp, R.E. (2001) Advances in determination of a high-resolution three-dimensional structure of rhodopsin, a model of G-protein-coupled receptors (GPCRs). *Biochemistry* **40**, 7761–7772.
63. Huyghues-Despointes, B.M., Scholtz, J.M. & Baldwin, R.L. (1993) Effect of a single aspartate on helix stability at different positions in a neutral alanine-based peptide. *Protein Sci.* **2**, 1604–1611.
64. Huyghues-Despointes, B.M., Scholtz, J.M. & Baldwin, R.L. (1993) Helical peptides with three pairs of Asp-Arg and Glu-Arg residues in different orientations and spacings. *Protein Sci.* **2**, 80–85.
65. Wan, W.Y. & Milner-White, E.J. (1999) A natural grouping of motifs with an aspartate or asparagine residue forming two hydrogen bonds to residues ahead in sequence: their occurrence at alpha-helical N termini and in other situations. *J. Mol. Biol.* **286**, 1633–1649.
66. Feng, Y.H., Miura, S., Husain, A. & Karnik, S.S. (1998) Mechanism of constitutive activation of the AT_1 receptor: influence of the size of the agonist switch binding residue Asn (111). *Biochemistry* **37**, 15791–15798.
67. Noda, K., Feng, Y.H., Liu, X.P., Saad, Y., Husain, A. & Karnik, S.S. (1996) The active state of the AT_1 angiotensin receptor is generated by angiotensin II induction. *Biochemistry* **35**, 16435–16442.
68. Miura, S., Feng, Y.H., Husain, A. & Karnik, S.S. (1999) Role of aromaticity of agonist switches of angiotensin II in the activation of the AT_1 receptor. *J. Biol. Chem.* **274**, 7103–7110.

69. Porschke, D. & Eigen, M. (1971) Co-operative non-enzymic base recognition. 3. Kinetics of the helix-coil transition of the oligoribouridylic-oligoriboadenylic acid system and of oligoriboadenylic acid alone at acidic pH. *J. Mol. Biol.* **62**, 361–381.

Supplementary material

The following material is available from http://www.blackwellpublishing.com/products/journals/suppmat/EJB/EJB3441/EJB3441sm.htm

Table S1. Resonance assignments made using standard high-field 2D methods.
Table S2. List of NOEs.
Table S3. ^{13}C-NMR resonance assignments and chemical shifts.
Table S4. $^{3}J_{\mathrm{HN\text{-}H\alpha}}$ values.
Fig. S1. Ensemble-averaging cross-validation results against the number of conformers in the ensemble.